PERGAMON

Carbon 41 (2003) 713–722

CARBON

Influence of HNO_3 oxidation on the structure and adsorptive properties of corncob-based activated carbon

Abdel-Nasser A. El-Hendawy*

Physical Chemistry Department, National Research Centre, 12622 Dokki, Cairo, Egypt

Received 29 June 2002; accepted 18 January 2003

Abstract

An investigation of the impact of strong oxidation with HNO_3 on the porosity and adsorption characteristics of char and activated carbons, derived from corncobs, is presented. Texture parameters, as obtained from N_2 adsorption at 77 K, showed a considerable decrease in surface area of the activated carbons with enhanced pore widening. The extent of porosity modification was found to depend on the scheme of activation of the precursor, simple carbonization, steam pyrolysis, steam gasification of the char, or chemical activation with H_3PO_4. Surface-chemical changes were detected by FTIR spectroscopy, where absorption bands assigned to carboxyl, carboxylate, carbonyl, and phenolic groups were observed. A SEM study demonstrated the erosive effect of HNO_3, detected by the presence of disintegration of the carbon grains, with the porous structure probably containing very large macropores. As a consequence of the oxidation process, elemental analysis showed high contents of O, H and N, and TG confirmed that the weight loss distribution in the thermogram becomes slower at higher temperatures. The removal of phenol decreased as a result of the formation of oxygen functionalities. Mono-nitrophenols were adsorbed in smaller amounts than phenol, and *p*-nitrophenol showed a relatively higher uptake than the other two mono-nitrophenols, whereas the uptake of Methylene Blue was improved. Removal of Pb^{2+} from aqueous non-buffered solution was considerably enhanced by chemical oxidation, which may be related to pore widening, increased cation-exchange capacity by oxygen groups, and the promoted hydrophilicity of the carbon surface.
© 2003 Elsevier Science Ltd. All rights reserved.

Keywords: A. Activated carbon; B. Activation, Oxidation; C. Adsorption; D. Adsorption properties

1. Introduction

Activated carbons (ACs) are increasingly used for the removal of organic chemicals and metal ions of environmental or economic concern from both potable water and wastewater. Wood, lignite coal, coconut shell, and peat are some of the raw materials currently used to prepare activated carbons. However, there has been growing interest in producing activated carbons from agricultural and field wastes. Their advantages as carbon feedstocks include availability as renewable resources, low ash content, reasonable hardness, and their ability to produce granular activated carbons (GACs) of high adsorption capacity [1,2]. In activated carbon–liquid-phase interactions or for ACs used as supports for catalysts, the surface chemical properties of the solid play a significant role.

During their preparation, and particularly during cooling and storage, carbon materials are in contact with the ambient air and elements such as H and O are fixed on the surface, leading to oxygenated chemical functions. Accordingly, a carbon can exhibit basic or acidic pH values in aqueous dispersions; in general, the more acidic the dispersion the higher the oxygen content [3].

Oxygen surface groups are very common in activated carbons and they may be easily introduced by oxidation with nitric acid, hydrogen peroxide, potassium permanganate, ammonium persulphate, air, etc. A given treatment will modify the pore structure and the chemical nature of the surface of an activated carbon, the extent of the modification being a function of both the structure of the carbon and the oxidation treatment [4]. In general, the order of the extent of oxidation produced is $HNO_3 > H_2O_2 >$ air, and it is almost independent of the porosity of the treated carbon. Depending on the ability of the oxidizing molecules to diffuse into the carbon pores, the

*Tel.: +20-30-223-2515; fax: +20-2-337-0931.
E-mail address: elhendawy@yahoo.com (A.A. El-Hendawy).

0008-6223/03/$ – see front matter © 2003 Elsevier Science Ltd. All rights reserved.
doi:10.1016/S0008-6223(03)00029-0

surface groups introduced seem to be preferentially located where there is wide microporosity.

It is commonly known that the oxidation of activated carbons can significantly enhance the adsorption capacity of these adsorbents by improving their ion-exchange properties. This process also increases the adsorption capacity of the sorbents with respect to polar adsorbents, such as alcohols, organic acids, esters, etc. [5]. The oxidation of activated carbons leads to the formation of various functional groups such as carboxylic, phenolic, carbonyl, etc. on the surface [5–11].

Thus, the modification of the surface chemistry of ACs is recognized as an attractive route towards the novel application of these materials as adsorbents for both gas-phase and liquid-phase adsorbates, as well as their use as catalyst supports. While ACs are used for the adsorption of organic compounds, many studies have shown that they can also sequester metal ions from solution [12–15]. Metal uptake is assumed to be a function of the polar or acidic surface groups on the carbon caused by the different oxygen complexes [11,16].

The present study deals with the influence of strong oxidation with HNO_3 of a carbon precursor of plant origin, activated under different conditions, on its adsorption properties. Thus, it demonstrates the effect of this treatment on: (1) the porosity characteristics determined from N_2 adsorption isotherms; (2) the removal capacity of several mono-substituted phenols; (3) the adsorption efficiency for Methylene Blue; and (4) the uptake of lead ions from non-buffered aqueous solutions. The study examined the impact of the preparation scheme (steam activation in the conventional or in single-step routes, phosphoric acid, or simple carbonization) on the extent of modification of various adsorption processes.

2. Materials and methods

2.1. Materials

Five carbons were considered in this study; details regarding the conditions used for their preparation and characterization were reported earlier [17]. The raw material, dried and crushed corncobs, was carbonized in a N_2 flow at 500 °C (C500), followed by activation in steam/N_2 at 850 °C (CS850). Two samples were obtained directly from the raw precursor under steam pyrolysis at 600 °C (CS600) and at 700 °C (CS700), and one sample by chemical activation with 50% H_3PO_4 at 500 °C (CP-55). These carbons were subjected to liquid-phase oxidation with HNO_3 to determine the effect of surface modification of the carbons, obtained under different schemes, on their adsorption properties from solution towards various substrates.

2.2. Oxidation of carbon samples

Analar-grade 65% nitric acid ($M = 63.01$ g/mol, Riedel-de Haen) was used to oxidize the carbons under severe conditions. The oxidation process was carried out by adding 50 cm^3 of the acid to 5 g of the carbon placed in a conical glass flask. The mixture was heated at 60 °C on a hot plate with constant stirring for 1 h, then washed with distilled water, decanted and the solid dried at 110 °C in an air oven. The pH of the investigated samples in CO_2-free distilled water at ambient temperature was also determined by mixing 1 g of carbon with 20 cm^3 of water. The suspensions were also shaken overnight, filtered and the pH values of the supernatant solutions measured.

2.3. Determination of porous characteristics

This was performed by the adsorption of N_2 at 77 K with the aid of a conventional vacuum system. Before measuring the adsorption of N_2, the sample was subjected to degassing for 2 h at 200 °C at a final pressure of 10^{-4} Torr. Analysis of the isotherms was carried out by applying the α_s method to obtain various parameters: S^{α}, S_n^{α} (total and non-microporous surface areas) and the micropore volume (V_o^{α}) using the standard α_s data reported by Sellez-Perez and Martin-Martinez [18]. The total pore volume (V_p) was estimated from the volume of N_2 (as liquid) held at a relative pressure ($P/P°$) of 0.95, and the mesopore volume (V_{meso}) from the volume adsorbed between $P/P° = 0.1$ and 0.95. The average pore radius was calculated from $\bar{r} = 2V_p/S^{\alpha}$ (nm).

2.4. Thermogravimetric (TG) and elemental analysis

Thermogravimetric analysis was performed on two samples: CP55 and its oxidized form $CP55_{(ox)}$. About 10 mg of each sample were heated from 25 to 1000 °C in flowing N_2 gas (purity 99.998 vol%; flow rate 50 cm^3/min). A Perkin-Elmer 7 series thermal analysis system was used with a heating rate of 10 °C/min to 1000 °C. The results display both TG and differential TG (DTG) tracings. Elemental analysis of the same samples was carried out using a VARIO EL ELEMENTAR apparatus.

2.5. FTIR spectra and SEM

The unoxidized and oxidized carbons were examined using Fourier transform infrared (FTIR) spectroscopy. Discs were prepared by first mixing 1 mg of powdered carbon with 500 mg of KBr (Merck; for spectroscopy) in an agate mortar, then pressing the resulting mixture successively under a pressure of 5 tons/cm^2 for 5 min, and at 10 tons/cm^2 for 5 min, under vacuum. The spectra of the samples were recorded between 4000 and 400 cm^{-1} using a Mattson 5000 spectrophotometer. Scanning elec-

tron microscopy was performed on two samples, CP55 and its oxidized form $CP55_{(ox)}$, using a SEM-type Jeol JSE-T20 system at a magnification of $\times 500$.

2.6. Adsorption from solution at 298 K

For batch experiments the tested carbons were milled and sieved to a particle size of <50 μm, and the carbon/substrate suspensions were placed in brown stoppered glass bottles and shaken overnight at room temperature. This scheme was followed when testing the removal capacity for phenol and the mono-substituted nitrophenols (*o*-, *m*-, *p*-). In each case, 50 mg of the powdered carbon was mixed with 50 ml of phenol solution (1 g/l). The residual concentration was monitored with a computerized Vis–UV spectrophotometer (Shimadzu) at wavelengths of 271, 351, 273 and 316 nm (phenol, *o*-, *m*- and *p*-nitrophenols).

The adsorption isotherms of Methylene Blue (BDH) were determined by mixing 50 mg of the powdered carbon with 50 ml of MB solution of varying concentration. The stoppered glass bottles were shaken for 24 h, and the filtered residual dye was analyzed by measuring its absorbance at 670 nm using the same spectrophotometer.

Adsorption isotherms of Pb^{2+} from unbuffered solutions of $Pb(NO_3)_2$ were determined by mixing 50 mg of the powdered carbon with 100 ml of Pb^{2+} solution of varying concentration, and shaking for 24 h. The residual metal was estimated, in the filtered solution, using an atomic absorption spectrometer (Perkin-Elmer Model 2380).

Analysis of the adsorption isotherms of MB and Pb^{2+} was performed by applying the linear Langmuir and Freundlich model equations:

$$\frac{C_e}{X_e} = \frac{1}{K_L X_m} + \frac{1}{X_m} \cdot C_e \quad \text{(the Langmuir equation)}$$

$$\log X_e = \log K_F + \frac{1}{n} \log C_e \quad \text{(the Freundlich equation)}$$

where C_e and X_e are the amounts of substrate in solution and on the solid (adsorbent), and K_L, K_F and n are equation constants. The monolayer capacity, X_m, was estimated for both solutes from the respective slopes of the Langmuir plots.

3. Results and discussion

3.1. Textural variations accompanying HNO_3 treatment

The N_2 adsorption isotherms are shown in Fig. 1. In general, they exhibit a mixed-type I+II of the BDDT classification with a small increase at higher relative pressure. This indicates that the oxidized carbons studied were mainly micro- and mesoporous in character with a minor presence of wider pores where capillary condensation occurred. Satisfactory α_s plots were obtained for the five investigated samples. Fig. 2 shows a straight line extrapolating to the origin and another linear region beyond $\alpha_s = 1.0$ with a considerable slope corresponding to the non-microporous surface area [19]. The α_s plot of the oxidized char $C500_{(ox)}$, in particular, exhibits two bending points, a downward or negative deviation at $\alpha_s < 0.8$, which may indicate the presence of a primary and secondary micropore filling mechanism [19], and an upward deviation (indicating multilayer formation and condensation in meso-macropores) beyond $\alpha_s = 1.1$. The estimated texture parameters are summarized in Table 1 for both the HNO_3 oxidized and the non-oxidized carbons. Different modifications of the porosity of activated carbons under the action of nitric acid treatment have been reported [4–7,9,20–22]. Some authors observed small changes, whereas others reported degradation of the porous structure with a considerable decrease in most textural parameters. The loss of total surface area and micropore volume was assumed to be related to the fixation of oxygen groups at the entrance and on the walls of micropores. These oxygen functional groups increase the weight of the treated activated carbon by as much as 6 to 13% [4]. This trend would be highly dependent on the starting carbon as well as the HNO_3 treatment conditions (acid/carbon ratio, initial acid strength, temperature, duration and refluxing process). The extent of oxygen–carbon group formation will naturally affect the accessibility of the adsorbate to the oxidized active carbon.

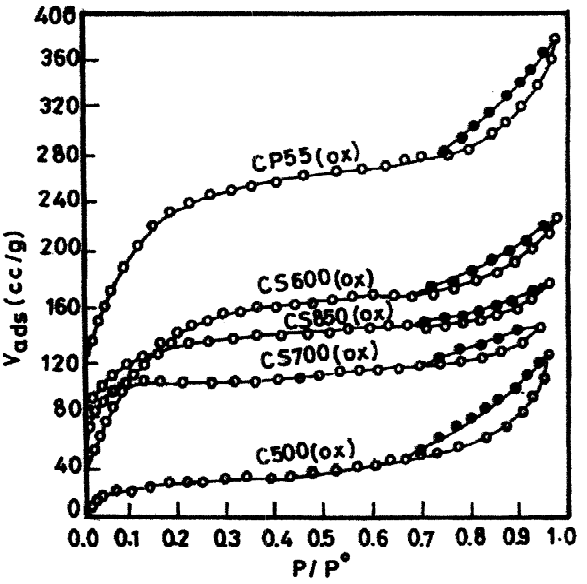

Fig. 1. Nitrogen adsorption isotherms of the investigated carbons at 77 K.

The data in Table 1 demonstrate that HNO_3 treatment of

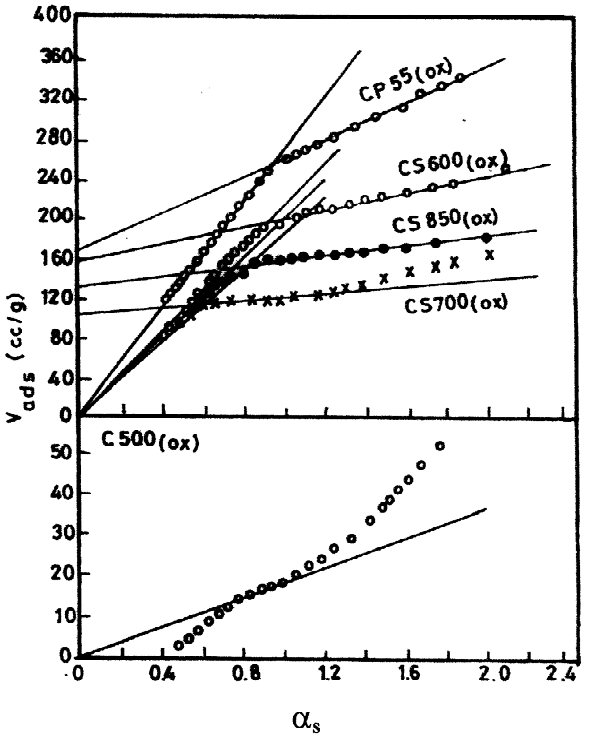

Fig. 2. α_s Plots of the N_2 adsorption isotherms of the investigated carbons at 77 K.

the activated carbons leads to an appreciable loss of the total surface area (from 13 to 25%) and a small increase in the mesopore volume with some widening of the average pore dimensions. Treatment of corncob-based char with boiling HNO_3 slightly increases its adsorption capacity, probably by dissolving some of the permeated inorganic matter and oxidizing deposited carbon that blocks pore openings, thus creating some micro- and mesoporosity. The four activated carbons exhibit an identical adverse effect of HNO_3, shown by a decrease in the total surface area accompanied by small changes in pore volumes in different size ranges (total, meso- and micropores). Accordingly, an apparent widening of the average pore radii is observed, indicating effective attack by HNO_3, particularly on micropores, by causing partial destruction of their structure [6], which would result in the loss of total surface area along with slight changes in the pore volume of the carbons. The erosive action of HNO_3 was also confirmed by scanning electron microscopy. Indeed, Fig. 3 clearly shows particle erosion and the disintegration of large grains into small grains, which might even produce very large macropores as a result of the distortion and/or the removal in adjacent micropores upon HNO_3 oxidation. The data in Table 2 show differences in the elemental analysis results, where the values for oxygen, hydrogen and nitrogen are much higher for the oxidized sample than for the corresponding non-oxidized sample, demonstrating the presence of a high density of acidic oxygen groups on the oxidized carbon surfaces as a consequence of oxidation treatment [4,5]. Thus, one can conclude that liquid-phase oxidation, especially when carried out under severe acidic conditions such as reported here, leads to the fixation of a large amount of oxygen functionalities on the carbon surface, with the simultaneous partial destruction or degradation of the porous structure of active carbons.

3.2. Thermogravimetric analysis (TG)

Fig. 4a and b presents the TG and DTG tracings for both CP55 and its oxidized form $CP55_{(ox)}$. It is clear that:

1. the weight loss up to 200 °C increases on oxidation, thereby indicating a higher affinity for water (increased hydrophilicity). The oxidized carbon shows many DTG peaks, demonstrating the successive loss and decomposition of various species with differing affinities at 110,

Table 1
Variation in the textural characteristics of the different carbons after HNO_3 treatment

Carbon	Slurry pH	S^{α} (m^2/g)	S_n^{α} (m^2/g)	V_p (cm^3/g)	V_o^{α} ($cm^3/g/$)	V_{meso} (cm^3/g)	$\bar{r}$ (nm)
C500	7.3	40	–	0.075	0.009	0.064	3.75
$C500_{(ox)}$	4.7	52	–	0.173	–	0.094	6.65
CS600	8.8	664	65	0.321	0.215	0.081	0.97
$CS600_{(ox)}$	6.2	577	101	0.359	0.203	0.158	1.24
CS700	9.2	850	108	0.430	0.252	0.121	1.01
$CS700_{(ox)}$	6.9	641	63	0.415	0.240	0.133	1.29
CS850	8.8	700	51	0.296	0.218	0.061	0.85
$CS850_{(ox)}$	5.8	540	65	0.286	0.205	0.093	1.08
CP55	3.8	923	368	0.629	0.249	0.324	1.36
$CP55_{(ox)}$	3.0	802	328	0.639	0.235	0.339	1.59

S^{α} and S_n^{α}, total and non-microporous surface areas from α_s plots; V_p, V_o^{α} and V_{meso}, total, micro and meso (0.95–0.1 $P/P°$) pore volumes; $\bar{r}$, average pore radius ($= 2V_p/s^{\alpha}$).

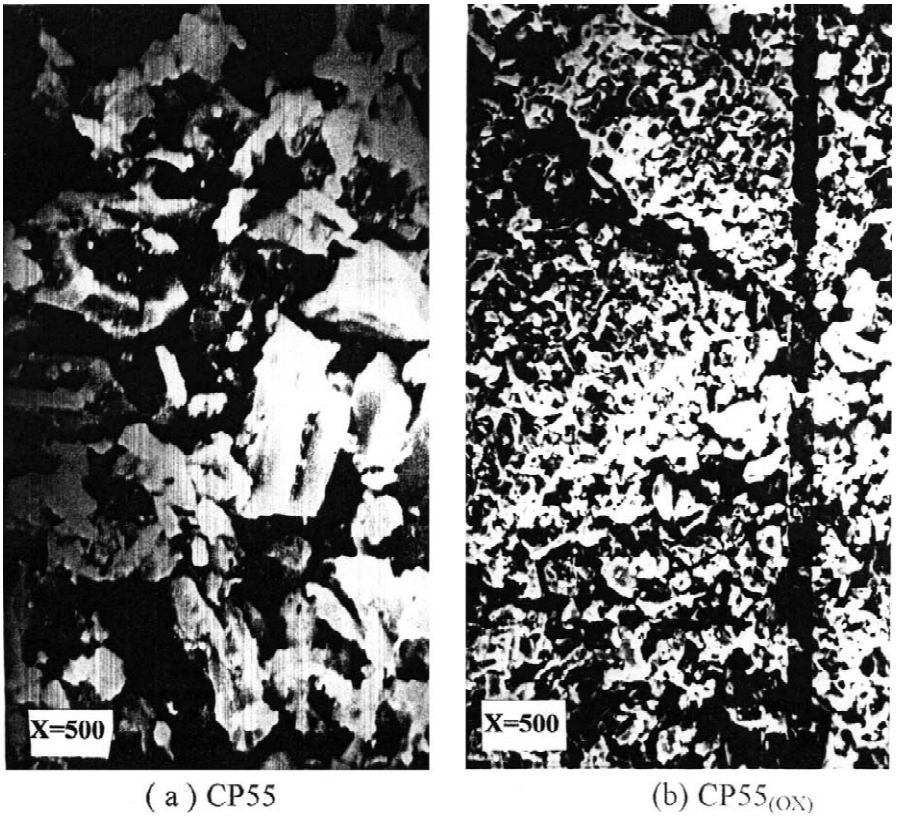

Fig. 3. Scanning electron micrographs of (a) CP55 and (b) $CP55_{(ox)}$.

270, 400, 570, and 740 °C (such as H_2O, CO_2, CO, etc.);

2. the oxidized carbon regularly loses much higher amounts up to 500 °C and degradation is induced throughout this range;
3. at 600 °C, both unoxidized and oxidized carbons attain a similar weight loss, viz. 63%;
4. between 600 and 700 °C, the unoxidized carbon exhibits a sharp weight loss (63–93%), whereas the oxidized carbon shows a more gradual loss (63–83%);
5. for the non-oxidized carbon a sharp loss in weight takes place with a high gradient of ~3.65%/min, whereas, within the same range, the oxidized carbon exhibits a much lower gradient of ~2.16%/min;
6. between 650 and 900 °C, the unoxidized and oxidized

Table 2
Elemental analysis of CP55 and its oxidized form $CP55_{(ox)}$

Carbon	Elemental analysis (wt%)			
	C	H	N	O (by difference)
CP55	77.50	2.28	0	20.22
$CP55_{(ox)}$	54.43	2.55	1.88	41.14

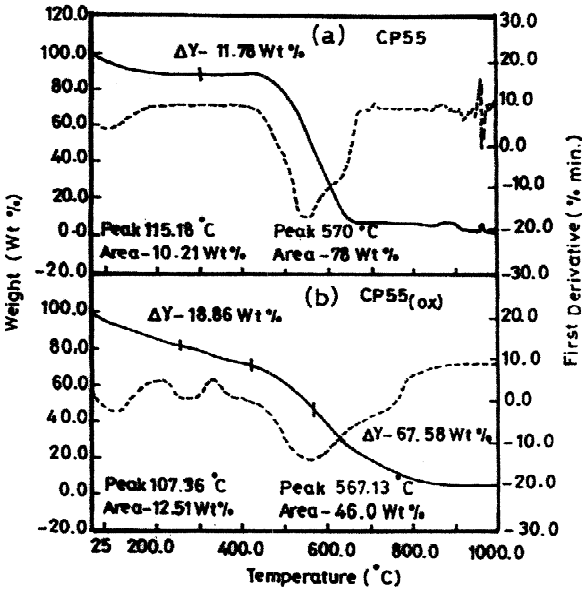

Fig. 4. TG and DTG curves for (a) CP55 and (b) $CP55_{(ox)}$.

carbons show reversed gradients of 0.47 and 0.9%/min, and at 900 °C a similar limiting weight loss is observed for both samples.

Thus from the weight loss shown by the DTG curves (Fig. 4), it can be deduced that wet oxidation of activated carbon with HNO_3 leads to an appreciable degree of functionality formation on the carbon surface. These functionalities become attached to such a high degree that their desorption, primarily as CO_2 and/or CO, requires high energy. Hence, the weight loss shown in the thermogram is distributed over a wide temperature range and the rate becomes slower only at a much higher temperature. These results corroborate the above observations concerning the effect of oxidation by HNO_3 on the surface chemical nature of active carbon. It can also be deduced from Fig. 4 that activated carbon is easily ignited under oxidizing conditions starting from 430 up to 700 °C. Oxidation with HNO_3 leads to initiation at the same temperature, but the HNO_3-preoxidized solid becomes more stable, showing a more gradual weight loss that extends to up 900 °C. It can be concluded from TG analysis that the weight changes monitored in flowing N_2 up to 1000 °C mainly reflect the presence of functional groups on the oxidized carbon surface and, at the same time, their successive decomposition or desorption. Moreover, it also reflects the relative thermal stability of the oxidized sample in relation to the non-oxidized sample, by preserving its carbon matrix and spreading the weight loss shown in the thermogram to much higher temperatures.

3.3. FTIR spectra

Fig. 5 shows the FTIR spectra of three representative carbons as well as their HNO_3-oxidized forms: the 500 °C char, the 700 °C single-step steam and the H_3PO_4-activated carbons. Observation of the absorption bands shows that the changes between the oxidized and non-oxidized carbons are mainly due to the formation of oxygen functionalities.

The FTIR absorption bands in the range above 3000 cm^{-1}, appearing as intense and broad peaks, are associated with the stretching vibrations of hydroxyl groups involved in hydrogen bonding, probably with the participation of water adsorbed on the carbon [10,23–25]. This absorption band is absent in the 500 °C char, probably due to its undeveloped structure and small surface area, as well as to its typically hydrophobic surface. This specific band is retained after oxidation particularly by the H_3PO_4 preactivated carbon with its more hydrophilic character and its much more developed internal structure. The shoulders observed at 2920 and 2360 cm^{-1} are usually ascribed to the presence of aliphatic compounds, and appear for the two activated carbons.

The most characteristic changes are observed within two ranges: 1820–1340 and 1300–1000 cm^{-1}. The former range is characteristic of the presence of C–O- and N–O-containing structures. The band centered at 1720 cm^{-1} is ascribed to the stretching vibrations of carboxyl groups on the edges of layer planes or to conjugated carbonyl groups (C=O in carboxylic acid and lactone groups) [10,24].

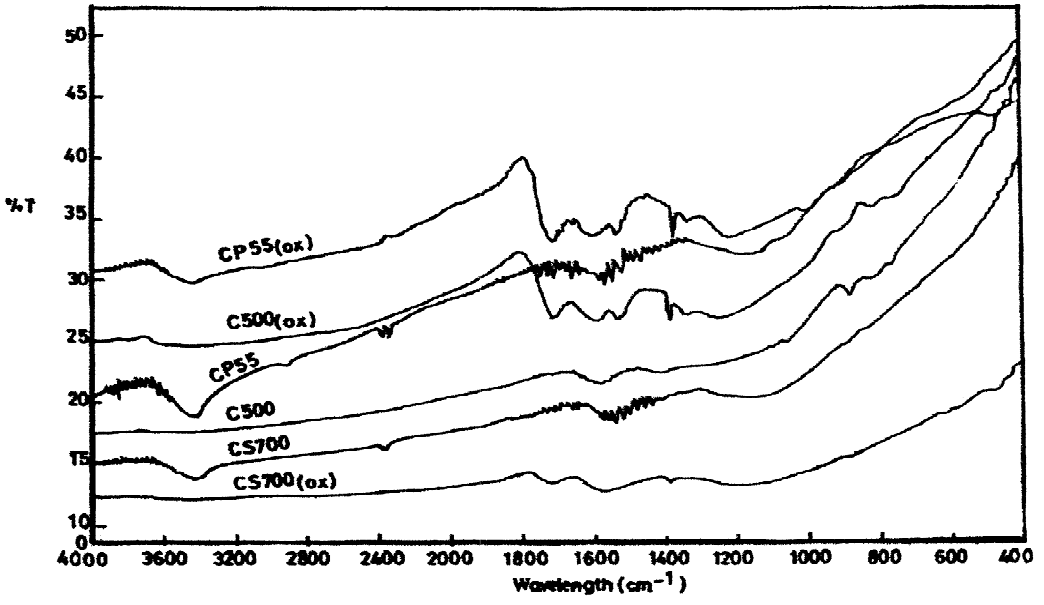

Fig. 5. Representative FTIR spectra for three oxidized samples in comparison with those for the parent non-oxidized carbons.

Absorption in the range 1600–1570 cm^{-1} is related to carboxylate groups (or ionized functions) [10,25]. The weak bands appearing at 1600, 1540, 1380, and 1340 cm^{-1} are all ascribed to the formation of, or to an increase in the already available, oxygen functionalities (highly conjugated C=O stretching, C–O stretching in carboxylic groups, and carboxylate moieties). These results indicate that HNO_3 treatment gave rise to a greater increase in C=O bonds in carboxylic acid and lactone groups.

The broad absorption within the range 1300–1000 cm^{-1} can be assigned to various C–O bonds, such as those in ethers, phenols and hydroxyl groups. Shoulder bands at lower wavenumbers (830, 760, 670 cm^{-1}) may be related to out-of-plane bending modes [25]. It has been suggested that, upon treatment with HNO_3, the changes in the intensity of the bands appearing between 1300 and 900 cm^{-1} are due to the formation of various oxygen surface groups and of structures containing N–O bonds (nitro-groups and nitrate complexes) as well as oxygen species mainly of a discrete nature [26]. This treatment was consequently associated with the increased surface acidity of the activated carbons [7,10,27,28] (Table 1).

3.4. Adsorption of selected phenolic compounds

It is well established that the sorption affinity of the surface of a carbon adsorbent depends essentially on: (a) the physical characteristics of its pore structure; (b) the chemical properties of the activated carbon surface; (c) the chemical structure of the sorbate; and (d) the characteristics of the surrounding solution. Increasing the number of oxygen functional groups increases the polarity of carbon surfaces and, therefore, their selectivity for water. Adsorbed water molecules or clusters may block carbon pores and reduce the sorption capacity for hydrophobic compounds [9,25], and enhance the uptake of phenolics and other polar adsorbents by oxidized carbons [5,9].

In the case of oxidized steam-activated carbons, the uptake of phenol is considerably reduced (by 32%) in comparison to that of the non-oxidized carbons (Table 3).

Table 3
Uptake of phenolic compounds by modified carbons (mmol/g)

Carbon	Phenol No.	Mono-substituted nitrophenols (NP)		
		o-NP	*m*-NP	*p*-NP
$C500_{(ox)}$	0.649 (na)	0.106	na	0.230
$CS600_{(ox)}$	1.202 (1.766)	0.230	na	0.374
$CS700_{(ox)}$	1.277 (1.893)	0.334	0.367	0.633
$CS850_{(ox)}$	1.191 (1.744)	0.385	0.406	0.467
$CP55_{(ox)}$	0.979 (1.021)	0.437	0.446	0.424

na, no adsorption. Values of phenol numbers for the parent unoxidized carbons in parentheses.

Acid-activated carbon $CP55_{(ox)}$ exhibits very little reduction in the uptake of phenol, whereas the oxidized C500 char generates considerable sites suitable for the adsorption of phenol. Mono-substituted nitrophenols are removed to a much smaller degree than non-substituted phenol. Except for sample $CP55_{(ox)}$, the removal of *ortho*- and *meta*-nitrophenols is the most inhibited, whereas *para*-nitrophenol is relatively the best removed among the three mono-substituted nitrophenols. In the presence of a charged and acidic surface, phenol, with a very weak acidic character, is strongly inhibited from ionization, and this enhances its relative affinity for the carbon surface in its molecular form. Nitrophenols, with a relatively higher acidity, show a selectively higher affinity for the medium, and thus reduced uptake. In addition, the oxygen functionalities formed at the entrance of the micropores, as well as the water clusters accumulating at these sites, hinder the uptake of the relatively bulkier nitrophenols. The most effective action seems to be related to *o*-nitrophenol, which may be due to its particular ability to form intermolecular hydrogen bonding structures.

It thus appears that the porous characteristics of the oxidized carbons play a minor role in determining the uptake of phenol and mono-substituted nitrophenols. For a given solution, the major role is played by the chemical properties of both the sorbent and the substrate in question. It should be remembered that, although carbon $CP55_{(ox)}$ possesses the best developed porosity, it shows the lowest uptake of phenol. This same carbon exhibits, in general, a similar removal capacity for the three nitrophenols as the other activated carbons.

3.5. Adsorption of Methylene Blue (MB)

Table 4 summarizes the Langmuir and Freundlich model parameters describing the adsorption isotherms (Fig. 6) of MB by HNO_3-treated carbons. In comparison with the non-oxidized carbons [17] the HNO_3-oxidized carbons show a relatively improved adsorption capacity for the dye (X_m); however, the dye occupies a smaller fraction of the total surface area (Table 4). In the case of the non-oxidized carbons it was assumed that the dye molecules lie flat on the carbon surface, covering an effective area of 1.2 nm^2/molecule. In contrast, on strongly oxidized and charged surfaces the MB molecules occupy a smaller area due to their vertical position or their flat position with an aggregation number of 2, and hence an effective area of 0.6 nm^2/molecule was assumed for coverage calculations [29]. Thus, the greater uptake of MB by the oxidized carbons cannot be ascribed to increased adsorption area, but rather to a greater compaction of MB molecules on the adsorbent surface. It seems safe to state that HNO_3 treatment of the activated carbons, including the char, promotes the uptake of MB, although it leads to some degradation of the carbon porosity.

Table 4
Adsorption parameters of Methylene Blue for the oxidized and non-oxidized carbons

Carbon	Langmuir model			Freundlich model		S_{MB}/S^{α}
	X_m (mmol/g)	S_{MB} (m^2/g)	K_L	K_F	n	
C500	na	–	–	–	–	–
$C500_{(ox)}$	0.225	81	0.065	14	2.6	1.769
CS600	0.314	227	0.108	40	6.8	0.342
$CS600_{(ox)}$	0.516	187	0.032	41	4.1	0.324
CS700	0.917	662	0.091	75	3.2	0.779
$CS700_{(ox)}$	1.198	433	0.027	100	5.0	0.676
CS850	0.722	521	0.092	69	4.7	0.744
$CS850_{(ox)}$	0.788	285	0.052	112	5.5	0.528
CP55	1.215	877	0.044	72	3.3	0.950
$CP55_{(ox)}$	1.804	652	0.061	199	5.7	0.813

na, no adsorption; X_m, monolayer capacity; S_{MB}, surface area covered by Methylene Blue; K_L, K_F and n, constants in Langmuir and Freundlich adsorption models; S^{α}, total surface area from α_s plots.

3.6. Uptake of Pb^{2+} from aqueous solution

Fig. 7 presents the adsorption isotherms for the uptake of Pb^{2+} from non-buffered aqueous solutions at 298 K. The calculated Langmuir and Freundlich equation parameters are given in Table 5. Predicted isotherms are also shown in Fig. 5 employing the estimated model parameters in the corresponding equations at selected equilibrium concentrations. Neither of the models could describe the adsorption isotherms for the uptake of Pb^{2+} from aqueous solution throughout the whole range of concentrations. The removal of Pb^{2+} is presumably governed by both the cation-exchange sites on the carbon surface and diffusion through the intricate internal porosity of the adsorbent.

Liquid-phase oxidation with HNO_3 greatly enhances the adsorption capacity of all carbons (up to three times). Even corncob char removed 0.691 mmol/g after oxidation, and metal uptake by all activated carbons is promoted relative to that of the untreated char. The best removal capacity is achieved by the H_3PO_4-activated carbon (444 mg/g to ~2.145 mmol/g). The surface covered by Pb^{2+} was calculated as proposed by Ferro-Garcia et al. [30]. In comparison to the parent activated carbons the adsorbed metal ions occupy a much higher ratio of the oxidized surface (i.e. a mean value of 0.58 as compared to the value for non-modified carbons of 0.21). Since the HNO_3-treated carbons showed reduced surface areas, this emphasizes the role played by the surface-chemical nature of the adsorbent. Intensely oxidized carbon surfaces thus possess more adsorption sites available for the sequestration of lead ions from aqueous solution. Such an induced greater affinity is evident upon comparison of the model adsorption parameters (Table 5), which are much higher than for the non-oxidized carbons. Metal ion uptake has been demonstrated to be a function of polar or acidic surface groups on the carbon surface and is favored by the presence of oxygen-containing functional groups and the electrostatic attraction of the metal for these sites [1,3,7,11]. The existence of surface oxygen functionalities was detected in this work, as well as being reported by several investigators following carbon surface modification with nitric acid. These acidic groups lead to very low point of zero charge [29] values and greatly increase the surface charge, which makes Pb^{2+} more accessible to the inner pores. It should be recalled that the surface oxygen groups enhance the hydrophilic character of the carbon surface, thus promoting metal adsorption and pore diffusion of the aqueous, and hydrated, lead ions.

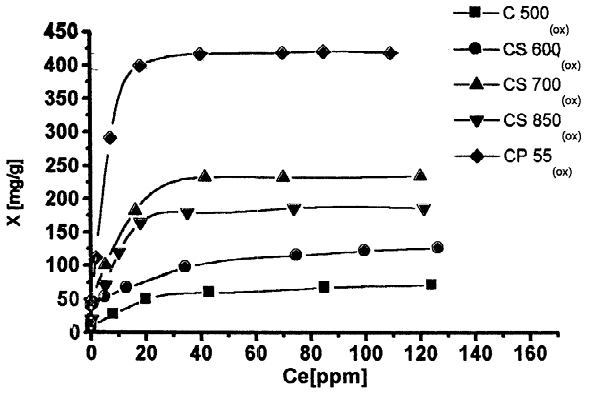

Fig. 6. Adsorption isotherms of Methylene Blue at 298 K.

4. Conclusions

Liquid-phase oxidation of char and activated carbons derived from corncobs with HNO_3 results in considerable modifications of their texture and adsorption properties. Corncob char of poor initial porosity showed a small enhancement in its total surface area and pore volume,

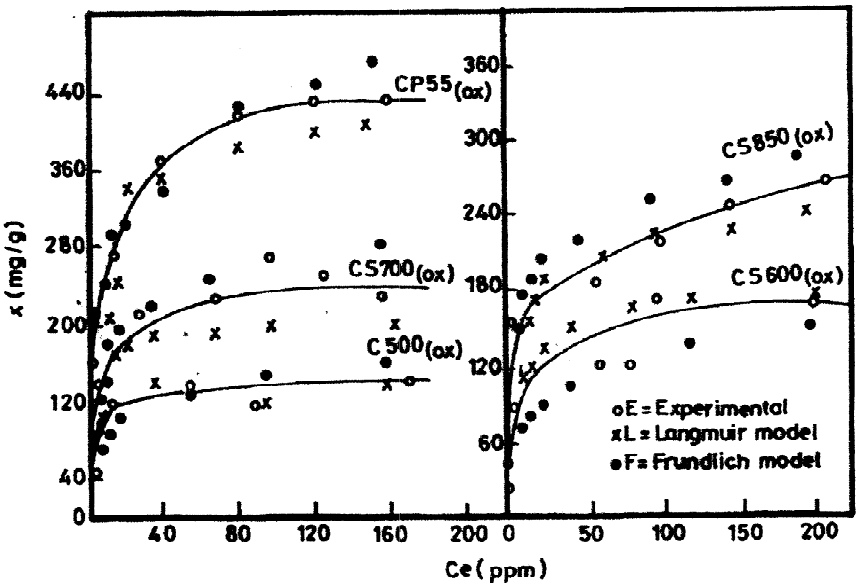

Fig. 7. Adsorption isotherms for the uptake of Pb^{2+} from aqueous solution at 298 K and the predicted isotherms.

whereas the structural features of activated carbons obtained under different conditions are adversely affected, and experience a loss of surface area. This may be related to the generation of bulky oxygen functionalities in narrow pore openings and the destruction of some micropores. TG analysis confirms that oxygen functional groups become so attached to the carbon surface that their desorption requires higher energy, and thus the TG weight loss spreads over a wide temperature range in the thermogram and becomes slower at much higher temperatures. Oxidation of the steam pre-activated carbons degraded their capacity for the removal of phenol, whereas the H_3PO_4-activated carbon is not affected due to its intrinsic highly developed porosity with abundant meso/macroporosity. *p*-Nitrophenol is generally adsorbed in greater amounts than either *o*- or *m*-nitrophenols, probably due to steric hindrance effects. Liquid-phase oxidation with HNO_3 promotes the removal capacity for Methylene Blue, in most cases as a consequence of pore widening. Considerable enhancement in the uptake of lead ions is observed for all carbons, including the char, which strongly indicates the role of the abundantly generated oxygen functionalities and the increase in the hydrophilicity of the carbon surface. The results point to the feasibility of the use of HNO_3-oxidized corncob chars for the removal of both organic and inorganic species from aqueous solution.

Table 5
Adsorption parameters for the uptake of Pb^{2+} from aqueous solution onto oxidized and non-oxidized carbon

Carbon	Langmuir model			Freundlich model		$S^{Pb^{2+}}/S$
	X_m (mmol/g)	$S^{Pb^{2+}}$ (m^2/g)	K_L	K_F	n	
C500	0.237	72	0.012	4.1	2.5	1.80
$C500_{(ox)}$	0.691	210	0.35	50.1	4.4	4.04
CS600	0.541	164	0.018	7.8	2.1	0.25
$CS600_{(ox)}$	0.816	249	0.15	50.1	5.0	0.43
CS700	0.652	197	0.049	40.7	5.1	0.23
$CS700_{(ox)}$	0.966	293	0.500	126	7.2	0.46
CS850	0.430	131	0.075	35.5	5.9	0.19
$CS850_{(ox)}$	1.130	343	0.177	126	6.4	0.64
CP55	0.695	211	0.084	4.4	1.8	0.23
$CP55_{(ox)}$	2.145	651	0.092	141	4.0	0.81

$S^{Pb^{2+}}$, surface area covered by hydrated lead ions; other parameters are defined in the footnote to Table 5.

References

[1] Johns MM, Marshall WE, Toles CA. J Chem Technol Biotechnol 1999;24:1037–44.
[2] Girgis BS, El-Hendawy AA. Microporous Mesoporous Mater 2002;52:105–17.
[3] Lahaye J. Fuel 1998;77:543–7.
[4] Molina-Sabio M, Munecas-Vidal MA, Rodriguez-Reinoso F. In: Rodriguez-Reinoso F et al., editor, Characterization of porous solids, vol. II, 1991, p. 329.
[5] Choma JM, Jaroniec W, Burakiewicz-Mortka J, Olejniczak K. Polish J Chem 1998;72:860–8.
[6] Choma JM, Burakiewicz-Mortka W, Jaroniec M, Li Z, Klinik J. J Colloid Interface Sci 1999;214:438–46.
[7] Biniak S, Szymanaki G, Swiatkowski A. In: Proceedings of the 9th International Conference on Coal Science, Essen, Germany, 1997, p. 1835.
[8] Carrasco-Marin F, Meuden A, Centeno TA, Stoeckli F, Moreno-Castilla C. J Chem Soc Faraday Trans 1997;93:2211–5.
[9] Karanfil T, Kilduff JE. Environ Sci Technol 1999;33:3217–24.
[10] Biniak S, Pakula M, Szymaanski GS, Swiatkowski A. Langmuir 1999;15:6117–22.
[11] Toles CA, Marshall WE, Johns MM. Carbon 1999;37:1207–14.
[12] Ferro-Garcia MA, Rivera-Utrilla J, Rodriguez-Cordillo J, Bautista-Toledo J. Carbon 1988;26:363–73.
[13] Corapicouglu MO, Huang CP. Water Res 1987;21:1031–44.
[14] Seco MP, Marzal P, Gabaldon C, Ferrer J. J Chem Technol Biotechnol 1997;68:23–30.
[15] Lee MY, Shin HJ, Lee SH, Park JM, Yang J-W. Sep Sci Technol 1998;33:1043–56.
[16] Leyva-Ramos R, Fuentes-Rubio L, Guerrero-Coronado RM, Mendoza-Barron J. J Chem Technol Biotechnol 1995;62:64–7.
[17] El-Hendawy AA, Samra SE, Girgis BS. Colloids and Surfaces A 2001;18:209–21.
[18] Selles-Perez MJ, Martin-Martinez JM. J Chem Soc Faraday Trans 1991;87:1237–43.
[19] Selles-Perez MJ, Martin-Martinez JM. Fuel 1991;70:877–81.
[20] Mok WS-L, Antal MJ, Szabo P, Varhegyi G, Zelei B. Ind Eng Chem Res 1992;3:1162–6.
[21] Park SH, McClain S, Tian ZR, Suib SL, Karwacki C. Chem Mater 1997;9:176–83.
[22] Menendez JA, Menendez EM, Garcia A, Igllsias MJ, Pis JJ. In: 216th ACS National Meeting, Boston, MA, 1998, p. 820, vol. 43.
[23] Vinke P, Van der Eijk M, Verbree M, Voskamp AJ, Van Bekkum H. Carbon 1994;32:675–86.
[24] Adib F, Bagreev A, Bandosz TJ. Environ Sci Technol 2000;34:636–92.
[25] Puziy AM, Poddubnaya OI. Mater Sci Forum 1999;:308–11.
[26] de la Puente G, Centeno A, Gil A, Grange P, Delmon B. In: 4th International Symposium on the Characterization of Porous Solids, Bath, UK, 1996, p. 327.
[27] Gil A, de la Puente G, Grange P. Microporous Mater 1997;12:51–61.
[28] Wang S, Lu GQ. Carbon 1998;36:283.
[29] Giles CH, D'Silva APD, Trivedi AS. In: Proceedings of the International Symposium on Surface Area Determination, Bristol, 1969, Butterworths, 1970, p. 317.
[30] Ferro-Garcia MA, Rivera-Utrilla J, Bautista-Toledo I, Mingarance MD. Carbon 1990;28:545–52.